AAPS PharmSciTech 2007; 8 (3) Article 60 (http://www.aapspharmscitech.org).

Characterization of β-Lapachone and Methylated β-Cyclodextrin Solid-state Systems

Received: December 22, 2006; Final Revision Received: February 26, 2007; Accepted: March 1, 2007; Published: July 27, 2007

Marcílio S. S. Cunha-Filho,[1] Bruno Dacunha-Marinho,[2] Juan J. Torres-Labandeira,[1] Ramón Martínez-Pacheco,[1] and Mariana Landín[1]

[1]Departamento de Farmacia y Tecnología Farmacéutica, Facultad de Farmacia, Universidad de Santiago de Compostela, Santiago de Compostela, Spain
[2]ED. CACTUS, Unidade de Raios X, Universidad de Santiago de Compostela, Santiago de Compostela, Spain

ABSTRACT

The purpose of this research was to explore the utility of β cyclodextrin (βCD) and β cyclodextrin derivatives (hydroxypropyl-β-cyclodextrin [HPβCD], sulfobutylether-β-CD [SBβCD], and a randomly methylated-β-CD [RMβCD]) to form inclusion complexes with the antitumoral drug, β-lapachone (βLAP), in order to overcome the problem of its poor water solubility. RMβCD presented the highest efficiency for βLAP solubilization and was selected to develop solid-state binary systems. Differential scanning calorimetry (DSC), X-ray powder diffractometry (XRPD), Fourier transform infrared (FTIR) and optical and scanning electron microscopy results suggest the formation of inclusion complexes by both freeze-drying and kneading techniques with a dramatic improvement in drug dissolution efficiency at 20-minute dissolution efficiency ($DE_{20\text{-minute}}$ 67.15% and 88.22%, respectively) against the drug ($DE_{20\text{-minute}}$ 27.11%) or the βCD/drug physical mixture ($DE_{20\text{-minute}}$ 27.22%). However, the kneading method gives a highly crystalline material that together with the adequate drug dissolution profile make it the best procedure in obtaining inclusion complexes of RMβCD/βLAP convenient for different applications of βLAP.

KEYWORDS: β-lapachone, antitumoral, cyclodextrin, inclusion complex, crystallinity, dissolution rate.

INTRODUCTION

β-lapachone (βLAP) is a naphtoquinone obtained on a small scale from South American trees of the families Bigoniaceae and Verbenaceae (Figure 1).[1] On a larger scale it can be produced following the method developed by Hooker and coworkers through cyclization of lapachol in sulphuric acid by nucleophilic attack of oxygen of the isoprenyl side chain and purification by further recrystallizations.[2]

Over the last few years β-lapachone has been reported to possess a wide range of pharmacological properties. It has antifungal, antiviral, antibacterial, anti-psoriatic, anti-inflammatory activities and also is an active agent against parasites such as *Trypanosoma cruzi*, the etiologic agent of Chagas disease.[3-8] However, its antineoplasic activity has certainly generated the greatest expectations on the molecule. In vitro and in vivo studies have shown that β-lapachone inhibits conventional therapy-resistant tumors, particularly the proliferation of neoplasms of slow cell cycle such as prostate, pancreatic, colon, and some ovarian and breast cancers.[9-12]

Despite its interesting potential applications, tests on humans and clinical trials have not yet been performed. The low water solubility of β-lapachone, 0.038 $mg \cdot mL^{-1}$, probably the cause of a low and erratic bioavailability, is the first problem to overcome in the development of dosage forms including the drug.[13]

Cyclodextrins (CDs) are cyclic oligosaccharides with lipophilic inner cavities and hydrophilic outer surfaces capable of interacting with a large variety of drugs giving noncovalent inclusion complexes that have been used extensively to improve solubility, dissolution rate, bioavailability, and stability.[14] Drugs such as β-lapachone, having aqueous solubility in micromole/liter range are good candidates for solubility enhancement through CD complexation.[15] Cyclodextrins have been shown to increase the solubility of β-lapachone as studied by Nasongkla and coworkers but the available information on this subject is extremely limited, particularly on solid systems.[16] The use of α, β, hydroxypropyl-β (HPβ), and γ CDs has been explored, concluding that βCD and especially HPβCD are useful in achieving an increase of water solubility up to 400-fold and overcoming the problem of parenteral administration.[16,17] However, with a view to use the oral route, the difficulty is maintained.

A limiting factor in selecting the appropriate CD for a formulation is the amount of complex to be administered. A dosage form for the oral route, a tablet for example, should not exceed 500 mg to 1 g. Since βLAP has a molecular weight of 242.3 and HPβCD of 1390, 100 mg of a complex

Corresponding Author: Mariana Landín, Departamento de Farmacia y Tecnología Farmacéutica, Facultad de Farmacia, Universidad de Santiago de Compostela, Santiago de Compostela, 15782, Spain. Tel: (34) 981 563100, ext 14876; Fax: (34) 981 549148; E-mail: mlandin@usc.es

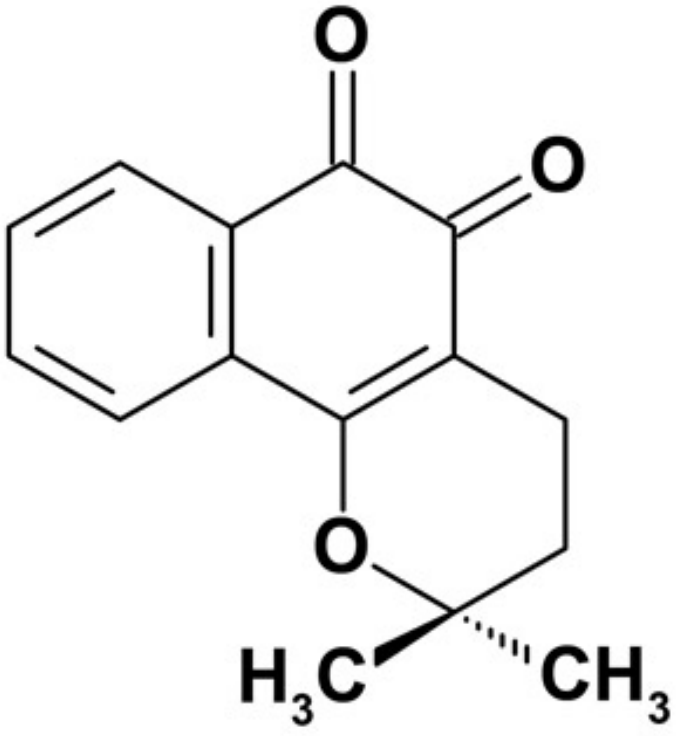

Figure 1. Chemical structure of β-lapachone (βLAP).

βLAP/HPβCD 1:1 contains ~14.8 mg of βLAP. It would be useful to find a CD derivative with a higher capacity of increasing βLAP solubility.[18]

On this basis, the main purpose of this research was to explore and compare, using a solubility diagram method, the utility of βCD derivatives to form inclusion complexes with βLAP in order to improve the capacity of increasing βLAP solubility. Four CDs have been selected: βCD and HPβCD, previously reported by Nasongkla and coworkers, and 2 additional βCD derivatives, sulfobutylether-β-cyclodextrin (SBβCD) and a randomly methylated-β cyclodextrin (RMβCD).[19]

Solid drug-RMβCD binary systems were prepared according to different techniques (physical mixing, kneading, and freeze-drying) and characterized by differential scanning calorimetry (DSC), X-ray powder diffractometry (XRPD), Fourier transform infrared (FTIR) spectroscopy, and optical and scanning electron microscopy (SEM) in order to achieve an improvement on βLAP dissolution properties useful for different applications.

Materials and Methods

Materials

β-lapachone (3,4-dihydro-2,2-dimethyl-2H-naphthol[1,2-b] pyran-5,6-dione; $C_{15}H_{14}O_3$; physical mixture [PM] 242.3) was supplied by Laboratorio Farmacêutico do Estado de Pernambuco/LAFEPE (Recife, Brazil). Purity estimated by DSC and high-performance liquid chromatography (HPLC) is 99.9%. βCD and RMβCD (degree of molar substitution 0.57) were kindly donated by Roquette (Barcelona, Spain); HPβCD (degree of molar substitution 2.7) was a Janssen Pharmaceutica (Beerse, Belgium) gift and SBβCD (degree of molar substitution 1.0) was a CyDex (Lenexa, KS) gift. All the βCD derivatives have an aqueous solubility higher than 20% (wt/vol). All other materials were of analytical grade. The solutions were prepared using distilled water and filtered through 0.22-μm Millipore filters (Millipore Corp, Billerica, MA).

Analytical Methods

A UV spectrophotometric method was developed for quantitative βLAP determination using a UV-visible spectrophotometer Agilent 8453 (Agilent Corp, Santa Clara, CA) with photodiode array detector at 257 nm. Calibration curve in water/ethanol (1:1 vol/vol) was made using standard solutions in the range of 2 to 10 μg mL^{-1}. The molar extinction coefficient found was 2.452×10^4 absorbance units.

No effect of the addition of cyclodextrins on the UV spectrum of βLAP solution was verified by comparison of βLAP and CDs/βLAP spectra for any of the CDs studied.

Drug chemical integrity on the liquid and solid systems was evaluated by HPLC analysis using a Waters M600 apparatus with photodiode array detector (Waters Corp, Milford, MA) equipped with a 5-μm C18 cartridge (125 × 4 mm) according to a previously reported method.[20]

Phase Solubility Studies

Phase solubility studies were performed according to the method reported by Higuchi and Connors.[21] Excess amounts of βLAP (~15 mg) were added to 3 mL of aqueous solutions containing increasing concentrations of CDs, in the range of 0% to 1% (wt/vol) for βCD; 0% to 2% (wt/vol) for HPβCD; 0% to 3% (wt/vol) for RMβCD; and 0% to 4% (wt/vol) for SBβCD. Suspensions were introduced into an ultrasound bath for 15 minutes and shaken in an oscillating water bath thermostatically controlled at 25°C for 7 days, enough time to guarantee the equilibrium, according to previous studies. Samples were filtered and appropriately diluted. βLAP concentration was determined spectrophotometrically. Experiments were performed in triplicate. The drug-CD association constants ($K_{1:1}$) were calculated, from the linear portion of the phase solubility diagrams assuming a 1:1 stoichiometry, using the following equation:

$$K_{1:1} = \frac{Slope}{S_0 \times (1 - Slope)} \quad (1)$$

where S_0 is βLAP water solubility in the absence of CD.

Preparation of Solid βLAP-RMβCD Systems

Preparation of Physical Mixture

A physical mixture (PM) of previously sieved granulometric fractions (100-250 μm) of βLAP and RMβCD in 1:1 molar ratio was obtained by mixing in a Turbula WAB T2C mixer (Willy A. Bachofen Corp, Basel, Switzerland) for 30 minutes.

Preparation of Kneaded Systems

The kneaded system (KN) was prepared from physical mixture in a mortar by slowly adding ethanol/water (1:1 vol/vol), in an amount of 20% wt/wt, and mixing until the homogeneous system was obtained.[22] Samples were dried in an oven at 40°C for 24 hours and powdered. A granulometric fraction (100-250 μm) was selected and characterized.

Preparation of Freeze-dried Systems

The physical mixture was dissolved in ethanol:water (1:1 vol/vol). The solution was frozen by immersion in liquid nitrogen and freeze-dried (FD) in a Labconco apparatus (Labconco Corp, Kansas City, MO). A 100–250 μm sieve granulometric fraction was collected for further characterization.

Solid βLAP-RMβCD System Characterization

X-ray Powder Diffraction

The X-ray powder diffraction patterns were collected using copper radiation (40 Kv, 30 mA), on a Philips PW 1729 diffractometer (Philips Corp, Netherlands) with Bragg-Brentano geometry, in the $2<2\theta<60$ range with a step size of 0.02º and counting time of 2 seconds per step. The microstructure study of the measured samples was determined through line profile analysis (LPA), which included a profile fitting stage to extract profile information from the powder diffraction peaks.

In order to compare the relative crystallinity of β-lapachone in the analyzed samples, the microstructural factor crystallite size was obtained using the analysis of the profile information by inverting the Warren-Averbach procedure.[23,24] A WinPLOTR software that implements the LPA method was used.[25]

On this basis it is possible to obtain

$$D_V = \lambda / \left(\text{Beta\_G(corrected)} * \cos\theta\right) \qquad (2)$$

where D_v is the volume-weighted domain size, Beta_G(corrected) is the Gaussian contribution to the integral breath after the instrumental broadening correction, λ represents the wavelength, and θ the peak Bragg angle. The instrumental profile component was determined experimentally by means of suitable profile standards.[26] As a further general assumption, we consider that the best polycrystalline analyzed sample with coherent diffraction crystallites is sufficiently small to provide an appropriate standard for the correction of the instrumental broadening.

Differential Scanning Calorimetry

Samples weighing 2 to 3 mg were placed in open aluminum pans and heated from 30°C to 250°C at a rate of $10°C \cdot min^{-1}$ using a temperature modulated DSC Q100 calorimeter (TA Instruments, New Castle, DE). Nitrogen was used as purge gas at a flux rate of $50\ mL \cdot min^{-1}$. Calibration of temperature and heat flow was performed with standard indium samples. All measurements were performed in triplicate. The percentage of βLAP in the original crystalline form (OCF) in the binary systems was calculated by the following equation[27]:

$$OCF = 100\frac{\Delta H_{BS}}{\Delta H_{PD}} \qquad (3)$$

where ΔH_{BS} is the fusion enthalpy of β-lapachone in the binary system and ΔH_{PD} is the fusion enthalpy of pure βLAP.

Fourier Transform Infrared Spectroscopy

Infrared spectra were obtained using a Bruker IFS-66V spectrometer (Bruker Daltonics Inc, Bremen, Germany). Samples were ground, mixed thoroughly with potassium bromide, and compressed in a hydraulic press. Thirty-two scans were obtained at a resolution 4 cm^{-1}.

Optical and Scanning Electron Microscopy

Optical morphological characteristics of the βLAP-CD systems were analyzed using an Olympus SZ60 (Opelco, Tokyo, Japan) optical microscope (OM) connected to a video camera Olympus DP12 (Opelco). The images were processed using Analysis version 3.2 (Analysis Software, Müster, Germany). Samples surface morphologies were examined using a LEO-435VP scanning electron microscopy (Leica Microsystems, Cambridge, UK). Particles were fixed on a brass stub using double-sided tape and gold coated in vacuum.

Dissolution Studies

In vitro dissolution studies were performed following Food and Drug Administration (FDA) specifications for poor soluble drugs using a United States Pharmacopeia (USP) dissolution apparatus 2 (paddle) (Turu Grau DT-6, Barcelona, Spain) at 75 rpm and 37°C (±0.5°C).[28]

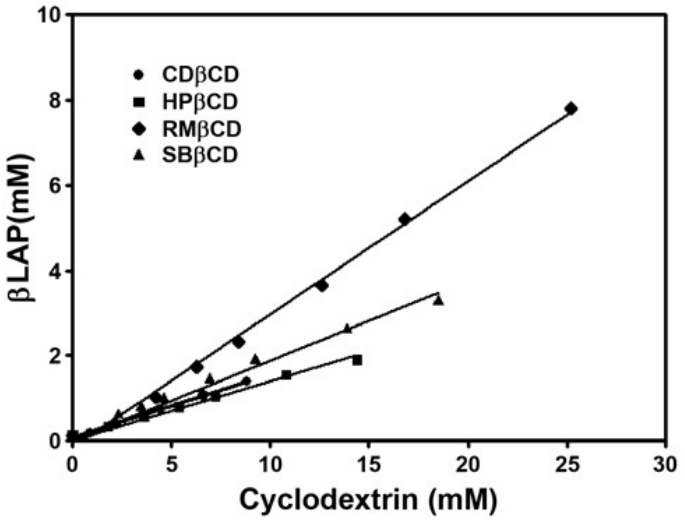

Figure 2. Phase solubility diagrams of β-lapachone (βLAP) as a function of cyclodextrin concentrations at 25°C in water.

In order to ensure sink conditions and increase the ability of the dissolution test to distinguish between formulations, the solubility of βLAP in water-containing surfactants were tested. A volume of 900 mL of aqueous solution of sodium lauryl sulfate at a concentration of 0.5% was selected as dissolution medium (solubility of βLAP in the dissolution medium selected was 0.163 mg mL^{-1}).[18]

Powdered samples of 50 mg of βLAP or equivalent amounts of each βLAP/CD system (particle size 100-250 μm) were tested. Powdered samples were submerged rapidly in the medium. At certain time intervals samples were collected, filtered through cellulose filters, and the concentration of drug dissolved determined by spectroscopy at 257 nm. For each binary system 3 replicates were tested. The dissolution profiles were evaluated and compared using the dissolution efficiency at 20-minute dissolution efficiency (DE_{20}) parameter.[29] The statistical analysis of the DE_{20} was performed by the 1-way analysis of variance (ANOVA) followed by least significant difference test using Statgraphics Plus version.[30]

Results and Discussion

Phase Solubility Diagrams

The effect of selected CDs on the aqueous solubility of βLAP (0.1264 mM) was evaluated using the phase solubility diagrams (Figure 2). The enhancement of βLAP solubility was highly dependent on the type of βCD. In all cases, the solubility of βLAP increased linearly as a function of cyclodextrin concentration over the studied concentration range with slopes lower than one (Table 1). Diagrams can be classified as A_L type and suggest a 1:1 mol:mol βLAP-CD stoichiometry, according to Higuchi and Connors.[21]

Association constants estimated for βLAP-βCD and βLAP-HPβCD were in agreement with previous data reported by Nasongkla and coworkers (1.23 10^3 M^{-1} for βCD and 0.94 10^3 M^{-1} for HPβCD).[16] The SBβCD and RMβCD, not yet evaluated in previous studies, had higher solubilizing effect on the drug than βCD and HPβCD. The association constant ($K_{1:1}$) obtained with RMβCD was almost 2 times higher than with the other βCD derivatives. The solubilization performance of RMβCD could be derived from the presence of the methyl groups, which can extend the hydrophobic region of the cyclodextrin cavity favoring and stabilizing the inclusion complexation of the βLAP molecule.[31] A similar effect occurs also with the hydroxypropyl or the sulfobutil ether groups but results suggest more favorable molecular interaction within the methyl groups.

As it was indicated earlier, for a solid oral formulation it would be useful to select the CD derivative with the highest capacity of increasing βLAP solubility. Therefore, the general characteristics of methylated βCD, especially its high aqueous solubility and low toxicity together with its higher efficiency for βLAP solubilization made RMβCD the candidate for inclusion in an oral solid dosage form.[32]

Preparation and Characterization of βLAP-RMβCD Systems

When a cyclodextrin and a potential guest are subjected to a treatment, there is no guarantee that a real inclusion complex will be produced. It has been reported that the product can be a mixture of complex, uncomplexed guest, empty cyclodextrin, and also different kinds of drug-CD interactions. As a consequence, a cautious physical-chemical analysis has to be performed to clarify the interactions between the components and its effects on the properties of interest.[22]

The chemical stability of the drug in the solid systems was evaluated by HPLC, finding neither chemical incompatibilities between components nor changes resulting from the stress of the process.

Table 1. Association Constants ($K_{1:1}$), Slopes and Correlation Coefficients (r^2) Obtained From the Phase Solubility Diagrams (n = 3)*

D	Slope	r^2	$K_{1:1}$ ($\times 10^3$ M^{-1})†
βCD	0.1484	0.9977	0.996 (0.020)
HPβCD	0.1270	0.9976	0.876 (0.026)
SBβCD	0.1712	0.9965	1.122 (0.027)
RMβCD	0.3127	0.9963	1.700 (0.024)

*βCD indicates β cyclodextrin; HPβCD, hydroxypropyl-β-cyclodextrin; SBβCD, sulfobutylether-β-CD; and RMβCD, randomly methylated-β-CD.
†Standard deviations appear in parentheses.

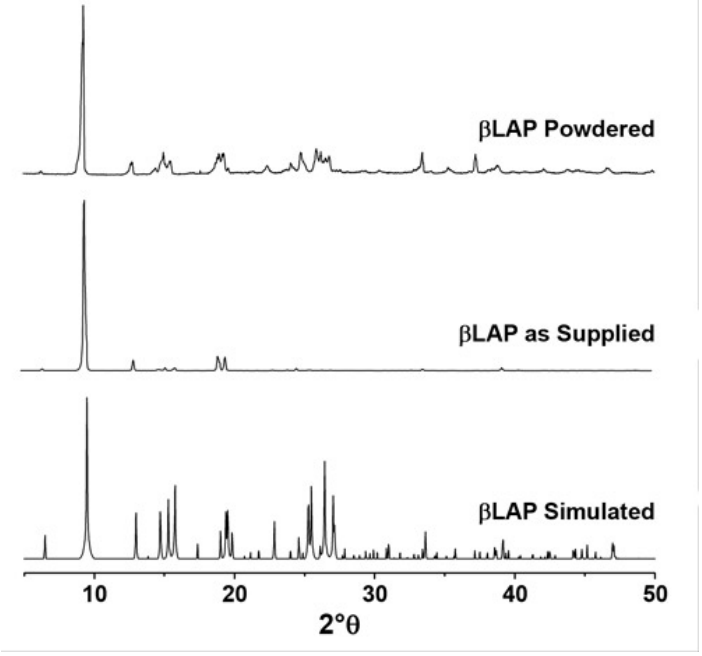

Figure 3. X-ray diffraction patterns of β-lapachone (βLAP) simulated; βLAP experimental as supplied and powdered.

X-ray Powder Diffraction

The possible XRPD patterns of βLAP are shown in Figure 3. βLAP presents a typical polycrystalline diffraction pattern, exhibiting a main sharp peak at 9.5 º2θ and secondary peaks at 13.05, 19.05, 19.59, 24.67, and 39.31 º2θ. The profile slightly changes in the βLAP powdered sample (100-250 μm). The preferred orientation variation on the analyzed crystallites could explain these differences because the relative intensity of the peaks showed changes. An ideal distribution of the crystallites can be seen at βLAP simulated pattern obtained from the single crystal data, where there is not preferred orientation at all.[33]

The XRPD pattern of RMβCD as supplied shows a diffuse pattern typical of an amorphous product. As can be seen in Figure 4, the pattern of the PM of βLAP-RMβCD can be obtained by the superimposition of pure component patterns. However, the kneading βLAP-RMβCD system XRPD profile presents a great change, involving new peaks, compared with the PM, which could be explained by crystallographic modifications performed during the formulation process. In order to understand such changes, RMβCD without drug was subjected to a kneading process under the same conditions. The product obtained ($RM\beta CD_{kneading}$; Figure 4) and RMβCD, as supplied, show completely different X-ray diffraction patterns, peak relative intensities, and shape, suggesting that the kneading process promotes the cyclodextrin crystallization. RMβCD has a random distribution of a few sterically small methyl groups that do not completely block the ability to form crystals on the contrary to other βCD derivatives.

Finally, the FD system seems to have the greatest pattern difference. The differences cannot be explained by the simple addition of the components, suggesting a clear interaction between the compounds.

In order to obtain the βLAP relative crystallinity from the analyzed samples, LPA was focused on the βLAP main peak. Figure 5 shows the normalized main peaks for the βLAP pure component and for the binary samples. Changes on the peak profile depending on the treatment can be seen. This finding confirms different microstructure properties. Assuming that the βLAP main peak was small enough to provide an appropriate standard for the correction of the instrumental broadening, it is possible to state that the FD system presents the lowest crystallinity with a Dv of 538.2 $Å^3$. The KN system shows a relative crystallinity of 987.7 $Å^3$, higher than the PM system with a Dv of 676.9 $Å^3$. This could be explained by the appearance of another kind of crystalline form for the KN system, which is different from the original and that makes this system more crystalline than the PM.

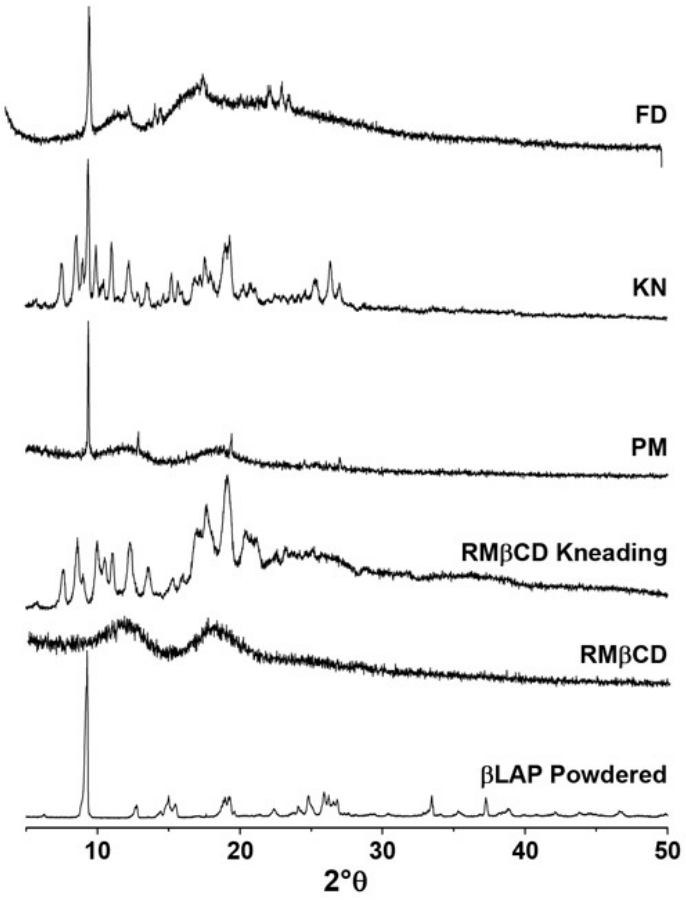

Figure 4. X-ray diffraction patterns of β-lapachone (βLAP) powdered; randomly methylated-β-CD (RMβCD) as supplied and kneading; and equimolar βLAP-RMβCD physical mixture (PM), kneading (KN), and freeze-dried (FD) systems.

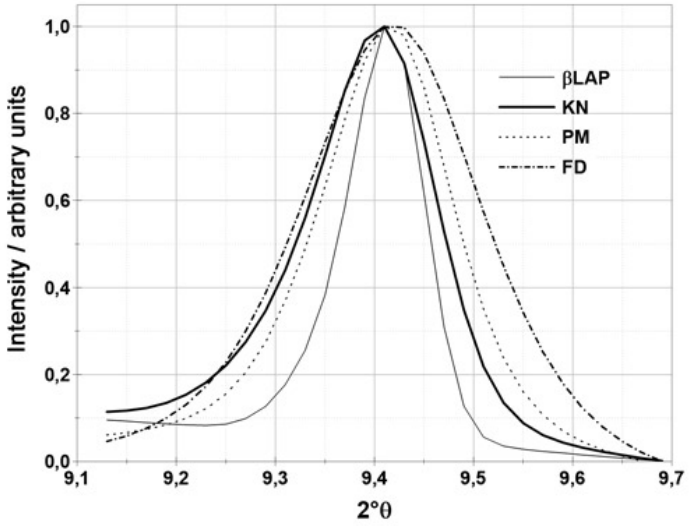

Figure 5. Normalized Bragg main peak for β-lapachone (βLAP) and for equimolar βLAP- randomly methylated-β-CD (RMβCD) physical mixture (PM); kneading (KN); and freeze-dried (FD) systems.

Differential Scanning Calorimetry Analysis

DSC analyses of raw materials and binary systems studied are shown in Figure 6 and Table 2. It can be seen that the βLAP DSC curve displays a sharp endotherm at 157.3°C, which is due to drug melting, characteristic of an anhydrous crystalline substance. RMβCD exhibits a broad endothermic effect ranging between 30°C and 149°C associated with water loss from inside the cavity.

Disappearance of the fusion peak of the drug is often interpreted as evidence of an inclusion complex formation. In the present study, the thermal profiles of all the binary systems showed the drug melting peak of βLAP, indicating the presence of unchanged drug in all the preparations, which is in agreement with XRPD data. The βLAP pattern in the PM was substantially unaffected in its shape and peak temperature, but a new small exothermic event was detected at 178.6°C (Table 2). This finding could be associated with a strong interaction between the CD and the melted drug and subsequent βLAP entrance into the empty CD cavity in an energetic favored process that decreased the energy of the system.[34] The phenomenon is still detectable and reproducible for the KN sample but not for the FD sample.

The DSC curves for KN and FD systems presented a slight shift in the melting peak of βLAP and an important reduction in the values of the associated enthalpy (Table 2). In addition, the KN system thermogram shows an extra-endothermic event possibly associated with a new crystalline form of the drug-CD complex as suggested by XRPD results.

An enthalpy reduction of the dehydration peak of $RM\beta CD_{kneading}$ with respect to the RMβCD as supplied can be seen (Figure 6), which could be attributed to the crystallization of the CD in a less hydrated form during the process of kneading (confirmed by XRPD and microscopy analysis).[27]

A large reduction in the dehydration enthalpy takes place in the FD system and could be explained by the replacement of water molecules inside the CD for drug molecules during the freeze-drying process.

The OCF parameter (Table 2) shows important reductions for FD (25%) and KN (49%) systems, indicating that residual original drug crystallinity is higher in the FD formulation than in the KN system. The combination of XRPD data and DSC suggests that the FD system presents a higher percentage of uncomplexed βLAP with a lower crystallinity degree. On the contrary, the KN system presents a lower percentage of uncomplexed drug but probably the procedure promotes the generation of new crystal phases with an additional associated endotherm at 160.3°C (Table 2).[35]

Fourier Transform Infrared Spectroscopy

The FTIR analysis is a useful technique to assess the interaction and the complex formation between drug molecules and CDs in the solid state. Shifts or intensity changes in the characteristic bands of pure substance are considered as evidence of the complex existence.[36] However, some changes are very subtle, requiring careful interpretation of the spectra.[22]

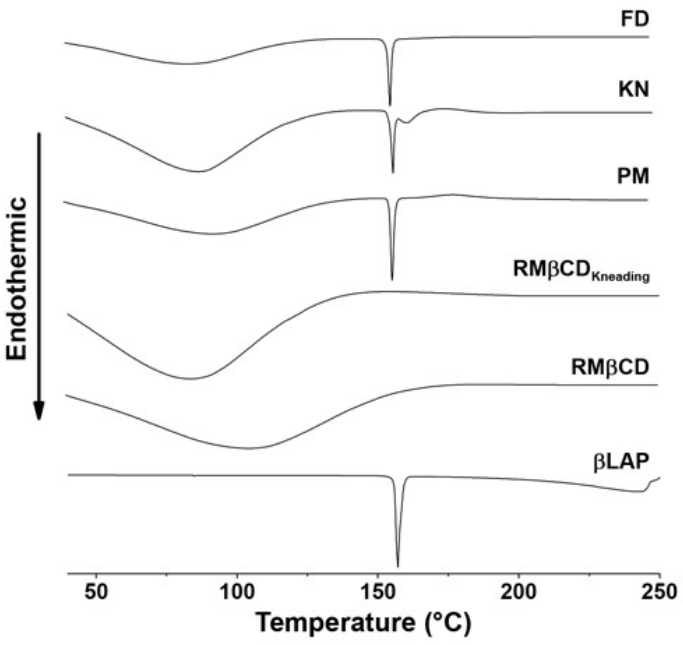

Figure 6. Differential scanning calorimetry thermograms of β-lapachone (βLAP); RMβCD as supplied and kneading; and equimolar βLAP-randomly methylated-β-CD (RMβCD) physical mixture (PM); kneading (KN); and freeze-dried (FD) systems.

Table 2. Thermal Data From DSC of βLAP; RMβCD as Supplied and Kneading; and Equimolar βLAP-RMβCD Physical Mixture; Kneading; and Freeze-dried Systems*

	Dehydration			Melting			Exothermic Peak			
Samples	Range ºC	Peak ºC	Enthalpy J g^{-1}†	Range ºC	Peak ºC	Enthalpy J g^{-1}‡	Range ºC	Peak ºC	Enthalpy J g^{-1}	OCF %
βLAP	—	—	—	151-162	157.3 (0.1)	103.2 (1.4)	—	—	—	100
RMβCD	30-149	91.0 (4.0)	376.3 (8.8)	—	—	—	—	—	—	—
RMβCD$_{kneading}$	30-149	90.6 (5.2)	233.9 (17.4)	—	—	—	—	—	—	—
PM	30-140	86.7 (1.5)	353.6 (11.5)	153-160	156.6 (0.1)	91.9 (0.1)	167-197	178.6 (0.4)	8.0 (0.4)	89.1 (0.1)
KN	30-138	83.9 (3.0)	368.1 (21.1)	152-157	155.7 (0.1)	53.3 (1.2)	166-188	174.1 (0.3)	4.0 (0.5)	51.6 (2.3)
				157-167	160.5 (0.2)	38.6 (2.8)				
FD	30-137	84.0 (0.7)	266.1 (20.8)	150-160	155.5 (0.1)	78.3 (0.7)	—	—	—	75.3 (0.7)

*DSC indicates differential scanning calorimetry; βLAP, β-lapachone; RMβCD, randomly methylated-β-CD; OCF, original crystalline form; PM, physical mixture; KN, kneading; and FD, freeze-dried. Standard deviations appear in parentheses.
†Per gram of RMβCD.
‡Per gram of βLAP.

Infrared spectra of βLAP, RMβCD, and the binary systems PM, KN, and FD are presented in Figure 7 and in Table 3.

The KN system shows a reduction in the band at 2978 cm^{-1} corresponding to C-H links of βLAP aromatic region compared with PM (Figure 7, Line 1), while the FD system shows the almost complete disappearance of this band.

In the region of 1700-1000 cm^{-1}, where RMβCD shows a broad band and βLAP did not overlap in the PM, the band corresponding to C=O group (Figure 7, Line 2) at 1695 cm^{-1} was clearly reduced in the FD system. Even for this preparation, bands corresponding to C-C links of aromatic region (Table 3, Line 4) presented a marked reduction in intensity and a shift to higher frequencies. In the region of C-O-C link (Table 3 and Figure 7, Lines 5 and 6), both KN and FD systems were affected by variations of the corresponding peak.

The results suggest that the inclusion of the drug inside the RMβCD cavity should take place by the aromatic group side (Figure 1). Although, the overlapping of drug-CD peaks in the methyl region of the molecule does not permit the rejection of the hypothesis of complexation on this side of the molecule.

Line 3 (Figure 7) represents the RMβCD characteristically O-H band linked with water.[18] A broadening of this band in the KN and FD systems could be explained by changes in the CD capacity of hydration, and it is additional evidence of a possible inclusion complex formation.

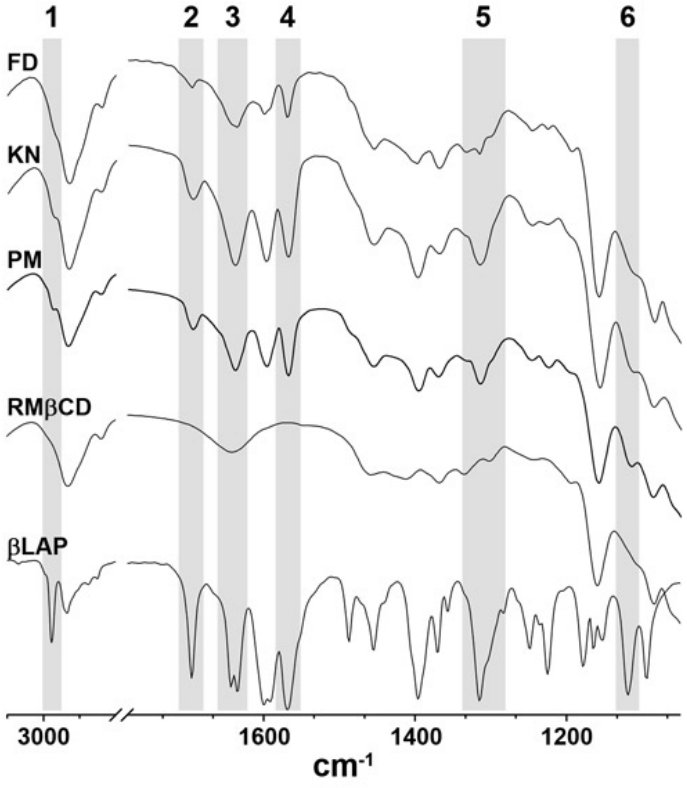

Figure 7. Fourier transform infrared spectra of β-lapachone (βLAP); randomly methylated-β-CD (RMβCD); and equimolar βLAP-RMβCD physical mixture (PM); kneading (KN); and freeze-dried (FD) systems.

Table 3. Fourier Transform Infrared Spectronomy Data of βLAP and Equimolar βLAP-RMβCD Physical Mixture, Kneading, and Freeze-dried Systems*

Line	Band	βLAP	PM	KN	FD
1	C-H_{ar}	2978	2978	—	—
2	C=O	1695	1694	1695	1695
4	C-C_{ar}	1600 1592	1597	1597	1599
		1569	1568	1568	1570
5	C-O-C	1315	1313	1315	—
6	C-O-C	1119	1115	—	—

*βLAP indicates β-lapachone; RMβCD, randomly methylated-β-CD; PM, physical mixture; KN, kneading; and FD, freeze-dried.

Optical and Scanning Electron Microscopy

Morphological changes can be employed as a tool for evidence of interaction between molecules and complex formation.[36,37] Selected photomicrographs by OM and SEM of the binary systems are presented in Figure 8. Orange crystals of βLAP surrounded by amorphous RMβCD particles are detectable in the PM system (PM1). There was not apparent interaction between both components in PM. On the contrary, significant modifications in color and shape were observed after kneading or freeze-drying. The KN system presented granular agglomerates of a strong orange color. It was not possible to distinguish between the 2 components (Figure 8, KN1). SEM (Figure 8, KN2) shows compact bulky particles as correspond to a crystalline material (eg, XRPD pattern, Figure 4). The FD system (Figure 8, FD1) showed a heterogeneous system with yellow particles dotted with orange crystals. SEM (Figure 8, FD2) presents a mixture of small amorphous particles and acicular crystals. Results confirm the XRPD and DSC data.

Dissolution Studies

Dissolution profiles of β-lapachone and equimolar binary systems βLAP-RMβCD as well as its dissolution efficiencies at 20 minutes are presented in Figure 9.

The increments in dissolution from inclusion complexes for different drugs have been explained on the basis of a higher energetic amorphous state/reduction of crystallinity, a lower interfacial tension between water-insoluble drug, and the dissolution medium induced by the CD and a greater water solubility of the complex.[37]

It is interesting to note that the PM of RMβCD with βLAP does not contribute significantly to an improvement of drug dissolution rate, indicating that the increment in local solubilization action of the CD does not explain the dissolution profile of the system.

FD and, especially KN, systems showed profiles with nearly 100% drug dissolved at 5 minutes. The comparison of drug release profiles was made by the calculation of dissolution efficiency parameter at 20 minutes. The ANOVA of the DE_{20} for the different systems showed significant differences among

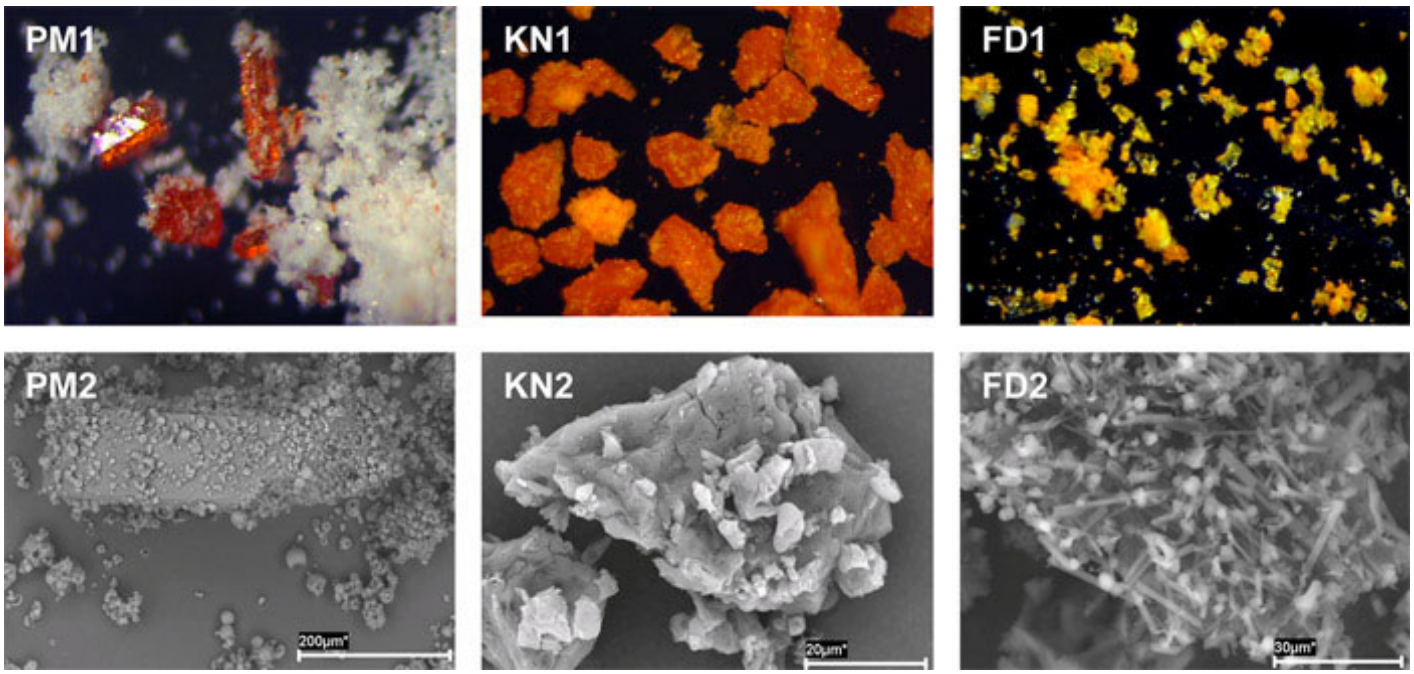

Figure 8. Photomicrographs by optical microscopy (1) and scanning electron microscopy (2) of equimolar β-lapachone (βLAP)-randomly methylated-β-CD (RMβCD) physical mixture (PM); kneading (KN); and freeze-dried (FD) systems using original magnification ×94.5.

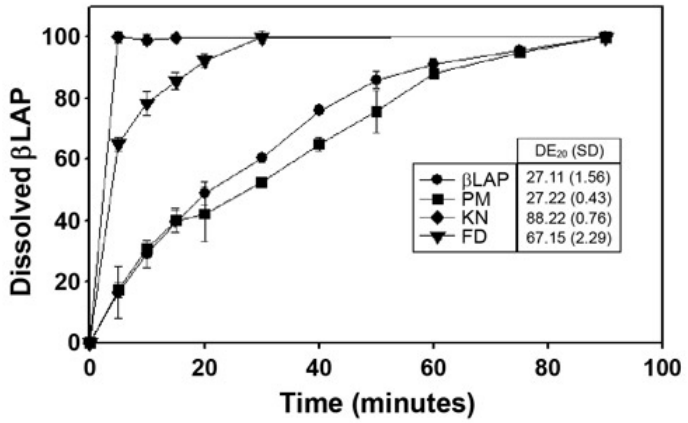

Figure 9. Dissolution profiles of β-lapachone (βLAP); equimolar βLAP-randomly methylated-β-CD (RMβCD) physical mixture (PM), kneading (KN), and freeze-dried (FD) systems in sink conditions, together with the corresponding mean values of the 20-minute dissolution efficiency (DE_{20}). SD indicates standard deviation.

formulations ($\alpha < 0.05$), and the least significant differences test presented 3 subsets. The dissolution rate was higher in the following order: βLAP PM < FD < KN.

The formation of readily soluble complexes by freeze-drying or kneading could be deduced in accordance with previous physicochemical characterization. A reduction in the degree of crystallinity is often associated with an increase in solubility.[27] However, in this case, the degree of crystallinity does not seem to be the only reason involved in the solubility change and probably the generation of new crystal phases (confirmed by XRPD) by the formulation process leading to distinctive microstructural properties is responsible for the different dissolution properties of the KN system. Small differences in the drug solubility rate between KN and FD systems should be related to the variability in the particle structure (Figure 8), which determines its wettability and deaggregation properties. Moreover, the crystallinity of KN system should improve manufacturability of the product.

CONCLUSION

In conclusion, the βCD derivatives studied, SBβCD and especially RMβCD, present high efficiency for βLAP solubilization. The results suggest that RMβCD possibly forms inclusion complexes by both freeze-drying and kneading techniques with a dramatic improvement in drug dissolution rate against the drug or the βCD/drug physical mixture. However, the kneading method gives a highly crystalline material that together with the adequate drug dissolution profile make it the best procedure in obtaining inclusion complexes of RMβCD/βLAP convenient for different applications of βLAP.

ACKNOWLEDGMENTS

This work was supported by Xunta de Galicia (PGIDIT04-BTF203011PR) and the Programme Alßan, the European Union Programme of High level Scholarships for Latin America, scholarship no. E04D043994BR.

The authors thank LAFEPE, Brazil, and Professor Dr Pedro Jose Rolim Neto, Federal University of Pernambuco, Brazil, for their kind gift of the βLAP. The authors are grateful also to Janssen Pharmaceutica, Roquette Freres, and CyDex for their generous donation of cyclodextrins.

REFERENCES

1. Burnett AR, Thomson RH. Naturally occurring quinones. XII. Extractives from *Tabebuia chrysantha* and other Bignoniaceae. *J Chem Soc C.* 1968;▪▪▪:850–853.

2. Hooker SC Jr, Shepard HW Jr, Walsh JG Jr, Connitt GH. Constitution of lapachol and its derivatives. *J Am Chem Soc.* 1936;58:1190–1197.

3. Guiraud P, Steiman R, Campos-Takaki G, Seigle-Murandi F, Simeon de Buochberg M. Comparison of antibacterial and antifungal activities of lapachol and b-lapachone. *Planta Med.* 1994;60:373–374.

4. Li CJ, Zhang LJ, Dezube BJ, Crumpacker CS, Pardee AB. Three inhibitors of type 1 human immunodeficiency virus long terminal repeat-directed gene expression and virus replication. *Proc Natl Acad Sci USA.* 1993;90:1839–1842.

5. Pereira EM, Machado T de B, Leal IC, et al. Tabebuia avellanedae naphthoquinones: Activity against methicillin-resistant staphylococcal strains, cytotoxic activity and in vivo dermal irritability analysis. *Ann Clin Microbiol Antimicrob.* 2006;5:5.

6. Muller K, Sellmer A, Wiegrebe W. Potential antipsoriatic agents: Lapacho compounds as potent inhibitors of HaCaT cell growth. *J Nat Prod.* 1999;62:1134–1136.

7. Tudan C, Jackson JK, Higo TT, Burt HM. The effect of inhibiting topoisomerase I and II on the anti-apoptotic response associated with pro-inflammatory crystals of calcium pyrophosphate dihydrate in human neutrophils. *Inflamm Res.* 2003;52:8–17.

8. Pinto CN, Dantas AP, De Moura KCG, et al. Chemical reactivity studies with naphthoquinones from tabebuia with anti-trypanosoma efficacy. *Arzneimittelforschung.* 2000;50:1120–1128.

9. Planchon SM, Wuerzberger S, Frydman B, et al. Beta-lapachone-mediated apoptosis in human promyelocytic leukemia (HL-60) and human prostate cancer cells: A p53-independent response. *Cancer Res.* 1995;55:3706–3711.

10. Li Y, Sun X, LaMont JT, Pardee AB, Li CJ. Selective killing of cancer cells by b-lapachone: Direct checkpoint activation as a strategy against cancer. *Proc Natl Acad Sci USA.* 2003;100:2674–2678.

11. Ough M, Lewis A, Bey EA, et al. Efficacy of beta-lapachone in pancreatic cancer treatment: Exploiting the novel, therapeutic target NQO1. *Cancer Biol Ther.* 2005;4:95–102.

12. Suzuki M, Amano M, Choi J, et al. Synergistic effects of radiation and beta-lapachone in DU-145 human prostate cancer cells in vitro. *Radiat Res.* 2006;165:525–531.

13. Jiang Z, Reddy DG, inventors. Pharmaceutical compositions containing b-lapachone or derivatives or analogs. PCT Designated States: Designated States W: AE, AG, AL, AM, AT, AU, AZ, BA, BB, BG, BR, BY, BZ, CA, CH, CN, CO, CR, CU, CZ, DE, DK, DM, DZ, EC, EE, ES, FI, GB, GD, GE, GH, GM, HR, HU, ID, IL, IN, IS,

JP, KE, KG, KP, KR, KZ, LC, LK, LR, LS, LT. US patent 7074824. February 13, 2003.

14. Rajewski RA, Stella VJ. Pharmaceutical applications of cyclodextrins. 2. In vivo drug delivery. *J Pharm Sci.* 1996;85: 1142–1169.

15. Loftsson T, Brewster ME. Pharmaceutical applications of cyclodextrins. 1. Drug solubilization and stabilization. *J Pharm Sci.* 1996;85:1017–1025.

16. Nasongkla N, Wiedmann AF, Bruening A, et al. Enhancement of solubility and bioavailability of beta-lapachone using cyclodextrin inclusion complexes. *Pharm Res.* 2003;20:1626–1633.

17. Wang F, Blanco E, Ai H, Boothman DA, Gao J. Modulating beta-lapachone release from polymer millirods through cyclodextrin complexation. *J Pharm Sci.* 2006;95:2309–2319.

18. Cao F, Guo J, Ping Q. The physicochemical characteristics of freeze-dried scutellarin-cyclodextrin tetracomponent complexes. *Drug Dev Ind Pharm.* 2005;31:747–756.

19. Davis ME, Brewster ME. Cyclodextrin-based pharmaceutics: Past, present and future. *Nat Rev Drug Discov.* 2004;3:1023–1035.

20. Soares da Cunha Filho MS, Alves FC, Alves GMC, Monteiro DB, Morais de Medeiros FP, Rolim Neto PJ. Beta-lapachone: Development and validation of analytical method for the new therapeutic antineoplastic alternative. *Rev Bras Farm.* 2005;86:39–43.

21. Higuchi T, Connors KA. Phase solubility techniques. *Adv Anal Chem.* 1965;4:117–212.

22. Hedges AR. Industrial applications of cyclodextrins. *Chem Rev.* 1998;98:2035–2044.

23. Balzar D, Audebrand N, Daymond MR, et al. Size-strain line-broadening analysis of the ceria round-robin sample. *Appl Cryst.* 2004;37:911–924.

24. Warren BE, Averbach BL. The effect of cold work in metals on powder pattern intensities. *J Appl Phys.* 1949;20:1066–1069.

25. Roisnel T, Rodriguez-Carvajal J. WinPLOTR: A Windows tool for powder diffraction patterns analysis Materials Science. Proceedings of European Powder Diffraction Conference; May 20-23, 2000; Barcelona, Spain. Stafa-Zurich, Switzerland: Trans Tech Publications; 2000:118–123.

26. Cline JP, Deslattes RD, Staudenmann JL. *Certificate SRM 660a.* Gaithersburg, MD: NIST; 2000.

27. Veiga MD, Diaz PJ, Ahsan F. Interactions of griseofulvin with cyclodextrins in solid binary systems. *J Pharm Sci.* 1998;87:891–900.

28. US Department of Health and Human Services. Guidance for Industry: Dissolution Testing of Immediate Release Solid Oral Dosage Forms, August 1997. Available at: http://www.fda.gov/cder/guidance/1713bp1.pdf. Accessed January 23, 2007.

29. Khan KA, Rhodes CT. Effect of compaction pressure on the dissolution efficiency of some direct compression systems. *Pharm Acta Helv.* 1972;47:594–607.

30. Fernández-Palacín F, López Sánchez MA, Muñoz Márquez MA, Rodríguez-Chía M, Sánchez-Navas A, Valero-Franco C. *Estadística Asistida por Ordenador. Statgraphics Plus 4.1.* Cádiz: Universidad de Cádiz; 2000.

31. Mura P, Furlanetto S, Cirri M, Maestrelli F, Corti G, Pinzauti S. Interaction of naproxen with ionic cyclodextrins in aqueous solution and in the solid state. *J Pharm Biomed Anal.* 2005;37:987–994.

32. Jacquet R, Elfakir C, Lafosse M. Characterization of a new methylated beta-cyclodextrin with a low degree of substitution by electrospray ionization mass spectrometry and liquid chromatography/mass spectrometry. *Rapid Commun Mass Spectrom.* 2005;19:3097–3102.

33. Cunha-Filho MS, Landin M, Martinez-Pacheco R, Dacunha-Marinho B. Beta-lapachone. *Acta Crystallogr C.* 2006;62:o473–o475.

34. Frooming K, Szejtli J. *Cyclodextrin in Pharmacy.* London, UK: Kluwer Academic Publishers; 1994.

35. Cabral Marques HM, Hadgraft J, Kellaway IW. Studies of cyclodextrin inclusion complexes. I. The salbutamol-cyclodextrin complex as studied by phase solubility and DSC. *Int J Pharm.* 1990;63:259–266.

36. Cirri M, Rangoni C, Maestrelli F, Corti G, Mura P. Development of fast-dissolving tablets of flurbiprofen-cyclodextrin complexes. *Drug Dev Ind Pharm.* 2005;31:697–707.

37. Fernandes CM, Teresa Vieira M, Veiga FJB. Physicochemical characterization and in vitro dissolution behavior of nicardipine-cyclodextrins inclusion compounds. *Eur J Pharm Sci.* 2002; 15:79–88.